

Formation mechanism of methane during coal evolution: A density functional theory study

Lina Zhang^a, Lixia Ling^b, Senpeng Zhao^b, Riguang Zhang^a, Baojun Wang^{a*}

*a. Key Laboratory of Coal Science and Technology (Taiyuan University of Technology),
Ministry of Education and Shanxi Province, Taiyuan 030024, Shanxi, China;*

b. Research Institute of Special Chemicals, Taiyuan University of Technology, Taiyuan 030024, Shanxi, China

[Manuscript received April 10, 2014; revised May 22, 2014]

Abstract

The formation mechanism of methane (CH₄) during coal evolution has been investigated by density functional theory (DFT) of quantum chemistry. Thermogenic gas, which is generated during the thermal evolution of medium rank coal, is the main source of coalbed methane (CBM). Ethylbenzene (A) and 6,7-dimethyl-5,6,7,8-tetrahydro-1-hydroxynaphthalene (B) have been used as model compounds to study the pyrolysis mechanism of highly volatile bituminous coal (R), according to the similarity of bond orders and bond lengths. All possible paths are designed for each model. It can be concluded that the activation energies for H-assisted paths are lower than others in the process of methane formation; an H radical attacking on β -C to yield CH₄ is the dominant path for the formation of CH₄ from highly volatile bituminous coal. In addition, the calculated results also reveal that the positions on which H radical attacks and to which intramolecular H migrates have effects on methyl cleavage.

Key words

coalbed methane; highly volatile bituminous coal; formation mechanism; density functional theory; kinetics

1. Introduction

CBM, which mainly consists of methane, is a major factor contributing to coal and gas outburst in mining [1,2]. The genetic type of CBM is divided into three categories: secondary biogenic gas, mixed genetic gas and thermogenic gas [3,4], in which the thermogenic gas is the main coalbed gas in China [5]. Most thermogenic gas is generated during the evolution of medium rank coal [6], in addition, the activity of highly volatile bituminous coal is very high [7].

Coal has made a breakthrough process to chemicals technology in China [8]. Thermal maturation of coal pyrolysis is the main process to form thermogenic gas which has been widely studied, and many researchers have attempted to develop methods to quantify the kinetic behavior of coal pyrolysis in the laboratory. Accordingly, the pyrolytic reactions of coal have received extensive attention, and excellent reports of the work performed in this area have been presented in the literatures. Thermogravimetric analysis is an important and

useful technique to analyze the change in coal samples during pyrolysis, which helps to provide information to obtain the relationship among species with increasing temperature [9–11]. It has been shown in the laboratory that a lower rank coal loses more weight at a lower pyrolysis temperature in comparison with a higher rank one. This is because lower rank coals contain fewer polyaromatic structures and they are richer in H. At the same time, coal pyrolysis is divided into three zones. The first represents some bond breaking reactions and the release of some light species ($\sim 490^\circ\text{C}$); the second is the primary pyrolysis phase (490–640 $^\circ\text{C}$), leading to the evolutions of tar, gas and char by further bond breaking; and the third is the secondary pyrolysis phase ($\sim 640^\circ\text{C}$), mainly resulting in CO and H₂ generation. Although the achievements are obvious, there is no progress in the formation mechanism of methane during the coal evolution. Besides, the cleavage of side chains and groups in the whole pyrolysis process [10,12] and the secondary decomposition of some gases and liquids [13] always occur to produce H radicals. Thus, there are a large number of

* Corresponding author. Tel: +86-351-6018239; Fax: +86-351-6041237; E-mail: wangbaojun@tyut.edu.cn

This work was supported by the Major Projects of National Science and Technology (Grant No. 2011ZX05040-005-002-001), the National Natural Science Foundation of China (Grant No. 21276171 and 21276003), the National Younger Natural Science Foundation of China (Grant No. 21103120) and China Postdoctoral Science Foundation (Grant No. 2012M520608).

H radicals during the coal evolution [14,15], which continually combine with other radicals. The existence of H radicals has important influence on coal pyrolysis. However, the kinetics of reactions as well as the effect of the H radical is not clear.

With the development of quantum chemistry, investigations on the reaction mechanism at a molecular level are widely conducted [16]. However, coal is a highly heterogeneous and complex material, making it difficult to generate meaningful representative structures. Up to now, a large number of coal related model compounds, which can partly reflect the local chemical properties of coal, have been investigated by density functional theory (DFT) method. To date, pyrolysis of toluene [17], ethylbenzene [18], benzoic acid, benzaldehyde [19], anisole [20], quinoline, isoquinoline [21], benzenethiol [22] and thiophene [23] have been studied. All results show that DFT is useful to describe the local chemical properties of coal using a local microstructure model. Liu et al. [24] have examined the pyrolysis of a brown coal model with a carboxylic group, and the formation mechanisms of CO₂ and H₂O have been demonstrated. Methane is mainly generated during the evolution of highly volatile bituminous coal, thereby the model of highly volatile bituminous coal is chosen to probe CH₄ formation.

In this work, the pyrolysis mechanism of highly volatile bituminous coal is studied to investigate CH₄ formation during coal evolution process in DFT. The processes of C–C bond cleavage as well as the formation and recombination of free radicals for CH₄ formation have been considered. All possible reaction paths have been studied in order to obtain the optimal path by analyzing activation energies. Also, the effect of H radicals on CH₄ formation has been evaluated.

2. Computational details

2.1. Computational method

All calculations were carried out in the framework of DFT using the Dmol³ program package in Materials Studio 5.5 [25,26]. All structures were geometrically optimized at the level of the generalized gradient approximation (GGA) with Perdew-Wang exchange-correlation functional (PW91) [27,28]. The atoms were treated with an all-electron basis set. The valence electron functions were expanded into a set of numerical atomic orbital by a double-numerical basis with polarization functions (DNP) [29]. Total self-consistent field (SCF) tolerance criteria, integration accuracy criteria and orbital cutoff quality criteria were set at medium. Multipolar expansion was set at octupole. In order to use the same orbitals for alpha and beta spins in calculations, spin unrestricted was chosen and the appropriate multiplicity was selected to perform a calculation on a specific spin state.

All reactants, products and possible intermediates in reaction paths were optimized and their single point energies (SPE) were determined at the same time. We chose the Complete LST/QST approach to search for transition states of reactions [30], thus getting accurate activation barriers of reac-

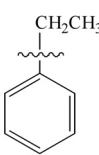
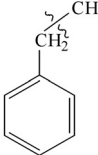
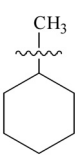
tions. The vibration analyses about the molecular structure of the species involved in the pyrolysis mechanism were carried out to validate the transition state, and transition state confirmation calculations were carried out on every transition state to confirm that transition states led to the desired reactants and products.

Bond dissociation energy (BDE) is an important thermodynamics parameter to characterize the molecular thermal stability. In order to evaluate the reliability of the selected calculation method and parameters, bond dissociation energies of C–C bonds contained in ethylbenzene and methylcyclohexane were calculated. For cracking reaction: R–X→R·+X·, the corresponding equation is as follows:

$$\text{BDE}(\text{R-X}) = {}_fH(\text{R}) + {}_fH(\text{X}) - {}_fH(\text{R-X}) \quad [31]$$

The results are listed in Table 1. We can see that calculated results are in good agreement with the experimental data [32]. Moreover, the value of BDE for ethylbenzene in the literature is 325.1 kJ·mol⁻¹ [33], which is very close to our results. Thus we can be sure of the reliability for the calculation method and parameters.

Table 1. Comparison of calculated and experimental BDE values of ethylbenzene and methylcyclohexane

Species			
$E_{\text{cal}}(\text{kJ}\cdot\text{mol}^{-1})$	415.1	323.2	371.1
$E_{\text{exp}}(\text{kJ}\cdot\text{mol}^{-1})$	419.2±4.2	319.7±7.1	377.0±7.5

2.2. Model analysis

The size influence of aromatic ring on the cleavage of C–C bond from alkyl side chain is negligible when the conjugated chemical environment of breaking bond does not be changed [34]. In addition, the division of model is feasible as Wang et al. [7] divide lignite into left and right to examine the thermochemical properties of different rank coals. Based on the theoretical background, it is reasonable to divide highly volatile bituminous coal (R) [35] into different partial models. R and a portion of partial models are shown in Figure 1. The investigation on methane formation mechanism mainly focus on the cleavage of side chains, so partial models which do not change the chemical environment of breaking bond can be used to conduct further study. The concept of bond order is a basic chemistry qualitative notion. It is often associated with bond strength, a measure of which is the bond dissociation energy [36]. Furthermore, the forecast of reaction mechanism depending on bond order has been studied [37]. In order to select reliable partial models, bond orders and bond lengths of R, A, B and C are investigated. The information on main breaking positions in four models is shown in Table 2. It shows that bond orders and bond lengths of A and

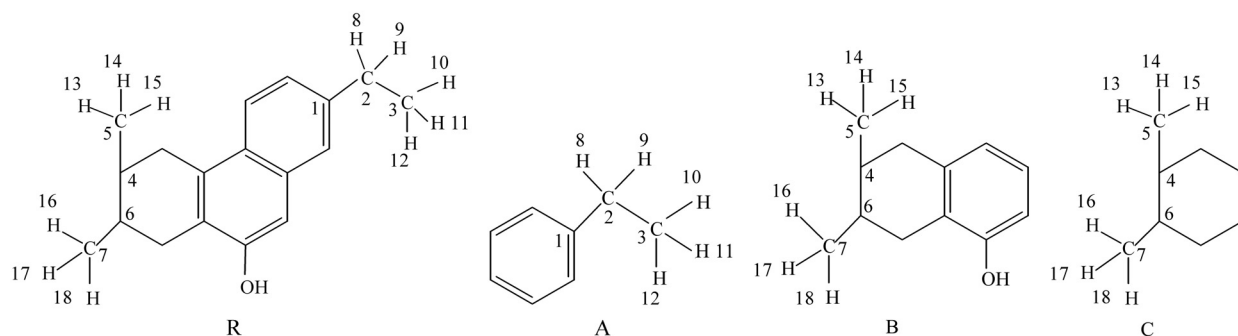


Figure 1. Models of highly volatile bituminous coal (R), ethylbenzene (A), 6,7-dimethyl-5,6,7,8-tetrahydro-1-hydroxynaphthalene (B) and 1,2-dimethylcyclohexane (C)

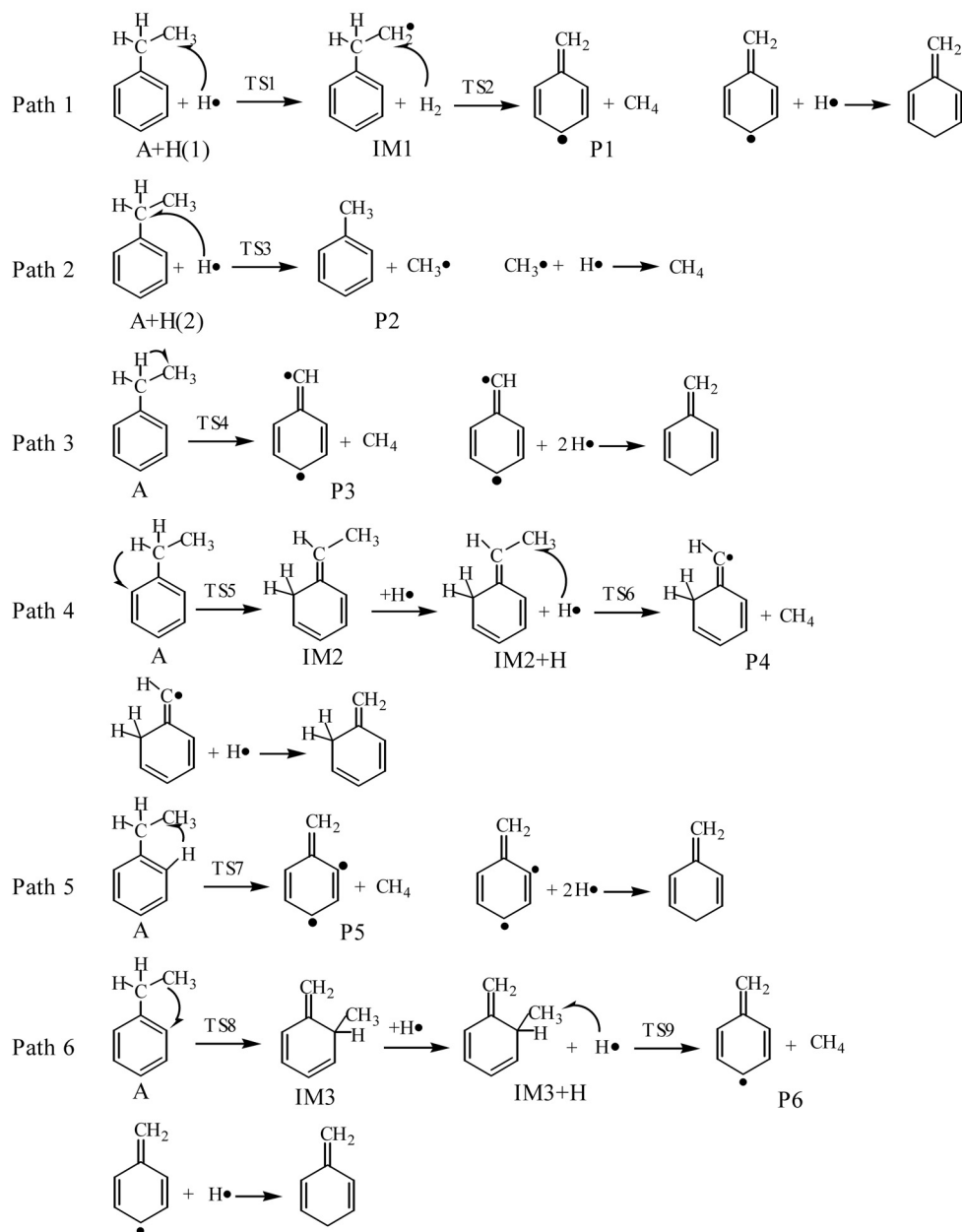


Figure 2. Formation mechanism of CH₄ for model A

B are similar to those of R. However, C has a large difference, because the conjugated chemical environment connecting with cyclohexane in model C has disappeared. Thus, the increased number of benzene ring in models A and B does not affect the results for C–C bond cleavage, while, the reduced number of benzene ring in models A and B can affect the

results. As a result, the highly volatile bituminous coal (R) can be modeled as ethylbenzene (A) and 6,7-dimethyl-5,6,7,8-tetrahydro-1-hydroxynaphthalene (B) to probe the formation mechanism of methane from highly volatile bituminous coal in this work. In this way the calculation efficiency could be significantly improved.

Table 2. Main bond orders and bond lengths of R, A, B and C

Bond	Bond order				Bond length (Å)			
	R	A	B	C	R	A	B	C
C1–C2	0.977	0.972			1.513	1.515		
C2–C3	1.003	1.002			1.525	1.526		
C2–H8	0.965	0.969			1.102	1.102		
C2–H9	0.965	0.965			1.102	1.103		
C3–H10	0.983	0.983			1.097	1.098		
C3–H11	0.977	0.978			1.099	1.099		
C3–H12	0.977	0.977			1.098	1.099		
C4–C5	0.980		0.979	0.979	1.533		1.533	1.535
C4–C6	0.959		0.960	0.956	1.541		1.544	1.551
C6–C7	0.996		0.995	0.992	1.528		1.528	1.529
C5–H13	0.975		0.975	0.976	1.098		1.097	1.097
C5–H14	0.976		0.979	0.978	1.098		1.097	1.098
C5–H15	0.971		0.970	0.969	1.098		1.098	1.098
C7–H16	0.981		0.981	0.980	1.098		1.098	1.099
C7–H17	0.970		0.970	0.974	1.099		1.099	1.098
C7–H18	0.980		0.980	0.981	1.099		1.099	1.098

3. Results and discussion

3.1. Model A

3.1.1. Reaction paths and structural parameters in model A

Three kinds of reactions for model A leading to the formation of CH₄ are analyzed in this part: an H radical attacks (Paths 1 and 2); the intramolecular H migration (Path 3 to Path 5) and intramolecular methyl migration (Path 6) followed by H-assisted steps, leading to CH₄ generation. The six different paths for the formation of CH₄ in model A are shown in Figure 2.

The reactants, intermediates, transition state structures and products for six paths are shown in Figure 3. The imaginary frequencies corresponding to transition states are listed in Table 3. In Path 1, an H radical initially attacks β -C, leading to the formation of IM1 via TS1 with an imaginary frequency of -1147.46 cm^{-1} . The C–H bond at β -C is broken and the bond length changes from 1.099 Å to 2.666 Å, as shown in Figure 3. Then the C–C bond is broken to yield CH₄ with the assistance of the generated H₂ via TS2, whose imaginary frequency is -1177.40 cm^{-1} . In this step, the length of C–C bond elongates to 3.772 Å from 1.484 Å. In Path 2, the α -C is attacked by an H radical followed by the cleavage of C–C bond and the formation of a methyl via TS3, which has the imaginary frequency of -942.73 cm^{-1} . The C–C bond changes from 1.526 Å to 3.593 Å in this step. Then, the methyl reacts with an H radical, which is a spontaneous elementary reaction without any activation barrier. Both Paths 3

and 4 both involve the migration of H at α -C. Path 3 is the migration of H to a β -C, resulting in CH₄ formation via TS4 with an imaginary frequency of -317.79 cm^{-1} . In this step, C–C bond elongates to 3.663 Å from 1.526 Å. In Path 4, the H migrates to benzene ring, leading to the formation of IM2 via TS5 with an imaginary frequency of -1073.06 cm^{-1} , which is consistent with our previous work [21]. The imaginary frequency of H at α -C migrating to benzene ring during the pyrolysis of quinoline and isoquinoline is -1056.13 cm^{-1} . In addition, the imaginary frequency of this step for toluene is -1020.00 cm^{-1} [17]. Then, CH₄ is yielded with the assistance of an H radical via TS6, with an imaginary frequency of -1318.63 cm^{-1} . In Path 5, the H migrates to a β -C, leading to the formation of CH₄ via TS7, whose imaginary frequency is -1606.68 cm^{-1} . In Path 6, we first investigate the migration of methyl to benzene ring, leading to the formation of IM3 via TS8 with an imaginary frequency of -211.18 cm^{-1} , after which CH₄ is yielded with the assistance of an H radical via TS9 with an imaginary frequency of -621.71 cm^{-1} .

Table 3. Imaginary frequency of each transition state of model A

Transition states	Imaginary frequency (cm ⁻¹)
TS1	-1147.46
TS2	-1177.40
TS3	-942.73
TS4	-317.79
TS5	-1073.06
TS6	-1318.63
TS7	-1606.68
TS8	-211.18
TS9	-621.71

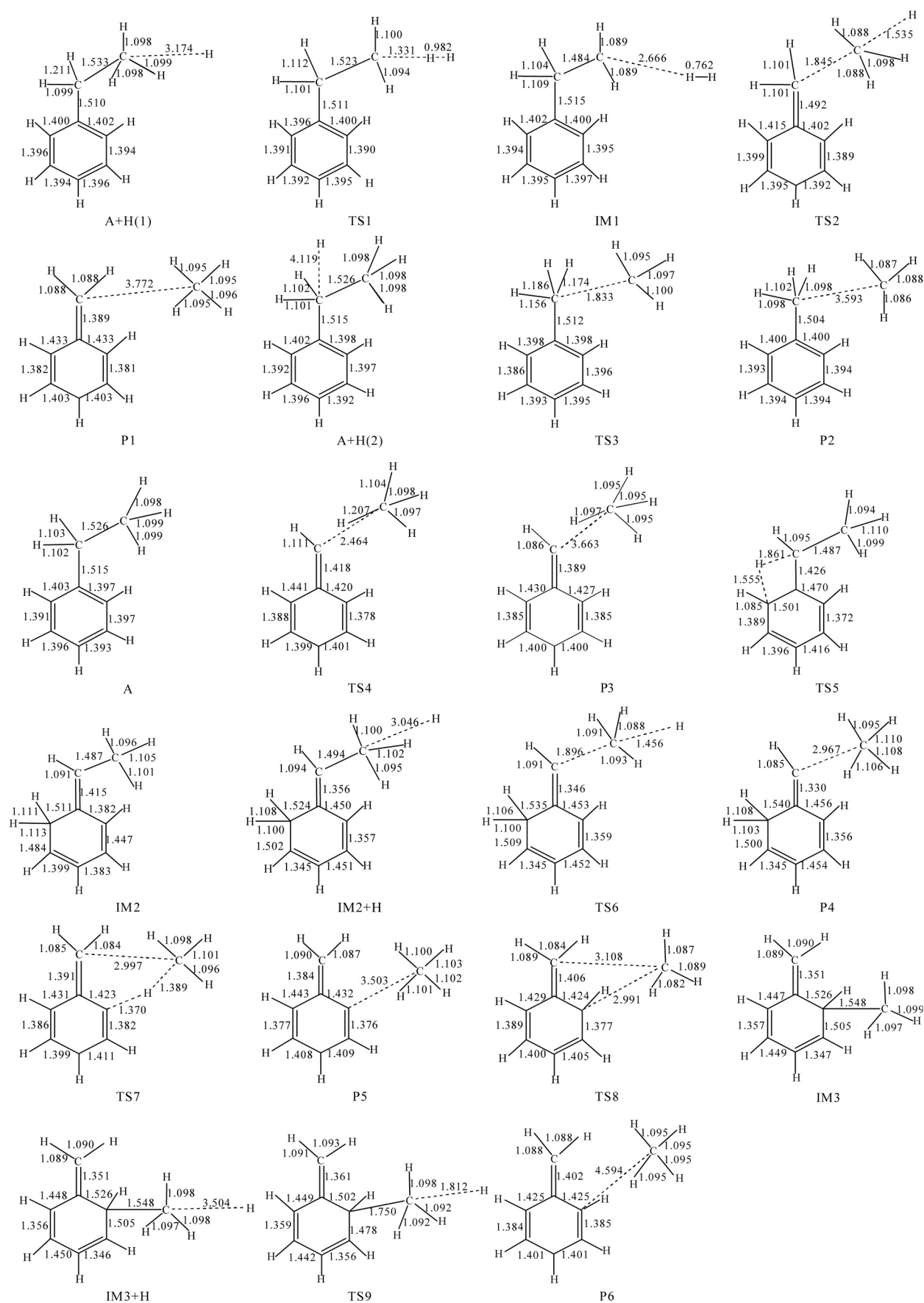


Figure 3. Optimized geometries of all reactants, intermediates, transition states and products during model A pyrolysis

3.1.2. Kinetic analysis of all paths in model A

In order to study the influence of temperature on methane generation, it is necessary to select an appropriate temperature to represent the low and high temperature, respectively. The low environment temperature for coal is 298.15 K [38], it is considered as low temperature for this study. The potential of methane conversion from coal is the highest at 875 K [39], and other hydrocarbons have completely released at this temperature [40,41]. As a result, 875 K is taken as high temperature. Furthermore, 298.15 K and 875 K were often used to represent the low and high temperature in the study of coal pyrolysis [17,23]. In summary, we investigate the kinetic analysis of reaction paths at 298.15 K and 875 K. According to the transition state theory, activation enthalpy ${}_rH_m^\ddagger$, activation entropy ${}_rS_m^\ddagger$, activation energy E_a and the rate constant k can be obtained from Equations (1)–(4), respectively.

$${}_rH_m^\ddagger = E_{\text{elec}}(\text{TS}) + H_m^0(\text{TS}) - E_{\text{elec}}(\text{R}) - H_m^0(\text{R}) \quad (1)$$

$${}_rS_m^\ddagger = S_m^0(\text{TS}) - S_m^0(\text{R}) \quad (2)$$

$$E_a = {}_rH_m^\ddagger + nRT \quad (3)$$

$$k = \frac{k_b T}{h} \left(\frac{p^0}{RT} \right)^{1-n} \exp \left[\frac{{}_rS_m^\ddagger}{R} \right] \exp \left[-\frac{{}_rH_m^\ddagger}{RT} \right] \quad (4)$$

where, T is the reaction temperature, n is the number of reactants, k_b , h , p^0 and R are Boltzman constant, Planck constant, standard atmospheric pressure and universal gas constant, respectively. ${}_rH_m^\ddagger$, ${}_rS_m^\ddagger$, E_a and the rate constant $\ln k$ of every elementary reaction at 298.15 K and 875 K are listed in Table 4.

Table 4. Activation enthalpy, activation entropy, activation energy and rate constant of six paths for model A

Elementary reactions		${}_rH_m^\ddagger$ (kJ·mol ⁻¹)		${}_rS_m^\ddagger$ (J·mol ⁻¹ ·K ⁻¹)		E_a (kJ·mol ⁻¹)		$\ln k$ (s ⁻¹)	
		298.15 K	875 K	298.15 K	875 K	298.15 K	875 K	298.15 K	875 K
Path 1	step 1	15.8	12.8	-29.1	-35.2	20.7	27.4	15.9	21.9
	step 2	124.9	115.0	-44.4	-63.9	129.8	129.5	-30.0	4.4
Path 2	step 3	176.8	170.5	-34.3	-46.9	181.8	185.0	-49.7	-1.2
Path 3	step 4	384.0	389.0	23.3	33.6	386.5	396.2	-122.7	-18.9
Path 4	step 5	341.0	344.4	11.1	18.5	343.5	351.6	-106.8	-14.6
	step 6	143.2	138.7	-40.3	-48.9	148.1	153.3	-36.8	3.0
Path 5	step 7	408.7	416.4	22.5	38.3	411.2	423.7	-132.7	-22.1
Path 6	step 8	384.6	392.0	39.4	55.5	387.1	399.3	-121.0	-16.7
	step 9	87.7	83.5	-34.1	-42.1	92.6	98.0	-13.7	11.4

As shown in Table 4, changes for activation energy can be ignored with the increase of temperature. Indeed, the activation energy is almost constant within a certain temperature range [42]. Raising the temperature will certainly increase the rate constants [43], which changes largely. Thus, the impact of temperature on methane generation is based on the comparison of rate constants. As a result, it can be concluded that the increase of reaction temperature favors the acceleration of CH₄ formation in model A. In addition, the activation energies for H-assisted paths are lower than others in the process of CH₄ formation, which is in agreement with the study of toluene pyrolysis [34]. Additionally, the theory of cation-radical pericyclic reactions also illustrates that the participation of cation radicals can lower the activation energy of reactions [44]. Step 2, the rate limiting step of Path 1, has an activation energy of 129.8 kJ·mol⁻¹, which is the lowest activation energy of all paths. It can be concluded that Path 1 is the dominant path yielding CH₄ in model A. In Path 2, H radical attacks α -C, which needs to overcome the activation energy of 181.8 kJ·mol⁻¹. Comparing Path 1 with Path 2, it can be suggested that H radical attacking on β -C are much easier than those on α -C. Path 3 is the migration of H at α -C to β -C with an activation energy of 386.5 kJ·mol⁻¹. While in Path 4, the migration of H at α -C to benzene ring needs an activation energy of 343.5 kJ·mol⁻¹. It is close to the direct

cleavage of H at α -C, which is 385.8 kJ·mol⁻¹ [33]. When β -C is attacked by an H radical after the migration, the activation energy is 148.1 kJ·mol⁻¹, which is higher than the path in which an H radical attacks β -C without the migration of H (129.8 kJ·mol⁻¹). A comparison of Paths 3 and 4 shows the migration of H at α -C to benzene ring is easier than that to β -C. In Path 5, the migration of intermolecular H at benzene ring to β -C has an activation energy of 411.2 kJ·mol⁻¹. Moreover, the activation energies of direct cleavage for H at benzene ring in the literature are 463.7 kJ·mol⁻¹ for toluene [45] and 487.1 kJ·mol⁻¹ for ethylbenzene [33]. Compared with Path 3, the migration of H at α -C to β -C is easier than that of H at benzene ring to β -C for reactions of intramolecular H migration to yield CH₄. In Path 6, the energy barrier of 387.1 kJ·mol⁻¹ is needed for the migration of methyl to benzene ring firstly, and then H radical attacks methyl with an activation energy of 92.6 kJ·mol⁻¹. The activation energy for the cleavage of methyl is 325.1 kJ·mol⁻¹ [33], which is lower than that for the migration of methyl (387.1 kJ·mol⁻¹). Therefore, Path 6 is not likely to occur in natural systems. Furthermore, the reaction order of model A can be obtained by analyzing the activation energy of each step, the order is Path 1 > Path 2 > Path 4 > Path 3 ≈ Path 6 > Path 5.

The kinetic analysis of model A indicates that the increase of reaction temperature favors the acceleration of CH₄

formation; H radical attacking on β -C is the dominant path leading to the formation of CH_4 ; H radical attacking on β -C is much easier than those on α -C; the migration of H at α -C to benzene ring is easier than that to β -C; and the migration of H at α -C to β -C is easier than that at benzene ring to β -C.

3.2. Model B

3.2.1. Reaction paths and structural parameters in model B

All possible paths of CH_4 formation in model B are analyzed in this part. All paths rely on the assistance of a coalbed H radical or intermolecular H molecule migration. Seven different paths in model B are studied, as shown in Figure 4.

The reactants, products and transition state structures are shown in Figure 5. The imaginary frequencies corresponding to transition states are listed in Table 5. Paths 1 and 2 are both H-assisted CH_4 formation. In Path 1, an H radical attacks a methyl connecting to an aromatic ring via TS1 with an imaginary frequency of -995.09 cm^{-1} . In this path, a C–C bond is broken, and the bond length changes from 1.528 Å to 3.735 Å, as shown in Figure 5. Similarly, in Path 2, an H radical attacks a methyl leading to the formation of CH_4 via TS2 with the imaginary frequency of -1154.41 cm^{-1} , and the C–C bond cleaves with the bond length changing from 1.532 Å to 3.409 Å. Although reactions for Paths 1 and 2 are very similar, the imaginary frequency difference exists in TS1 and TS2. This phenomenon is due to the influence of an –OH group. In addition, functional groups have effects on charge transfer, which have been reported in the literature [46]. The effects of different substituents on structural isomers and bonding have also been studied [47]. Paths 3 and 4 are both combi-

nations of H with a methyl at the same position of aromatic ring. The corresponding imaginary frequencies of TS3 and TS4, the transition states of Paths 3 and 4, are -119.28 and -639.77 cm^{-1} , respectively. In Path 3, the length of C–C bond elongates to 3.738 Å from 1.528 Å, and in Path 4, the corresponding C–C bond length elongates to 3.695 Å from 1.533 Å. Paths 5, 6 and 7 all involve methyl reacting with a neighboring H atom, which migrates to methyl via TS5, TS6 and TS7, respectively, leading to the formation of CH_4 . In Path 5, the imaginary frequency of TS5 is -1343.85 cm^{-1} and the C–C bond length changes from 1.533 Å to 4.007 Å. In Paths 6 and 7, the imaginary frequencies are -1728.33 cm^{-1} of TS6, and -1965.75 cm^{-1} of TS7. In addition, the C–C bond changes from 1.528 Å to 3.982 Å and 3.762 Å, respectively.

Table 5. Imaginary frequency of each transition state of model B

Transition states	Imaginary frequency (cm^{-1})
TS1	-995.09
TS2	-1154.41
TS3	-119.28
TS4	-639.77
TS5	-1343.85
TS6	-1728.33
TS7	-1965.75

3.2.2. Kinetic analysis of all paths in model B

The activation enthalpy ${}_rH_m^\ddagger$, activation entropy ${}_rS_m^\ddagger$, activation energy E_a and the rate constant $\ln k$ of every elementary reaction at 298.15 K and 875 K are listed in Table 6. Paths 5–7 are all elementary reactions.

Table 6. The activation enthalpy, activation entropy, activation energy and rate constant of seven paths for model B

Elementary reactions	${}_rH_m^\ddagger$ ($\text{kJ}\cdot\text{mol}^{-1}$)		${}_rS_m^\ddagger$ ($\text{J}\cdot\text{mol}^{-1}\cdot\text{K}^{-1}$)		E_a ($\text{kJ}\cdot\text{mol}^{-1}$)		$\ln k$ (s^{-1})	
	298.15 K	875 K	298.15 K	875 K	298.15 K	875 K	298.15 K	875 K
Path 1	140.5	139.4	-41.2	-43.0	145.5	154.0	-35.9	3.6
Path 2	140.3	137.2	-26.1	-32.1	145.3	151.7	-34.0	5.2
Path 3	387.4	391.1	30.4	38.4	389.9	398.3	-123.2	-18.6
Path 4	373.1	376.6	24.2	31.2	375.6	383.8	-118.2	-17.5
Path 5	428.0	434.9	61.0	75.4	430.5	442.2	-135.9	-20.2
Path 6	425.5	429.4	21.4	29.8	428.0	436.7	-139.6	-24.9
Path 7	531.1	537.4	41.4	54.6	533.6	544.7	-179.8	-36.8

The calculated results in Table 6 show that activation energies for Paths 1 and 2 (145.5 and $145.3 \text{ kJ}\cdot\text{mol}^{-1}$, respectively) are lower than others. However, the activation energy needed by direct cleavage of methyl for toluene is $417.3 \text{ kJ}\cdot\text{mol}^{-1}$ [45]. This is ascribed to the assistance of an H radical, which can significantly decrease the activation energy needed. The activation energies of Paths 3 and 4 are 389.9 and $375.6 \text{ kJ}\cdot\text{mol}^{-1}$, respectively. They both use a combination of H with a methyl at the same position of aromatic ring. For the combination of methyl with neighboring H atoms, the activation energies of Paths 5–7 are 430.5 , 428.0 and $533.6 \text{ kJ}\cdot\text{mol}^{-1}$, respectively. Comparing activation en-

ergies of Paths 1 with 2, Paths 3 with 4 and Paths 5 with 6, it can be concluded that there is little difference in activation energy between reactions in a similar chemical environment. The same results are obtained for heteronuclear single quantum coherence spectra of CN oligosaccharides for different lengths, which demonstrate that the resonance overlap is a result of the very similar chemical environment for these atoms [48]. It is evident that Path 7, with the highest activation energy, is the least favorable path. Similarly, the rate constants at different temperatures also show that the increase of reaction temperature favors the acceleration of CH_4 formation in model B. Meanwhile, the activation energy of each path in-

indicates that the reaction order for model B is Path 1 \approx Path 2>Path 3 \approx Path 4>Path 5 \approx Path 6>Path 7.

Kinetic analysis of model B indicates that the increase of reaction temperature favors the acceleration of CH₄ formation; an H radical attacking on an aromatic methyl is the dominant path leading to CH₄ generation; a similar chemical environment is consistent with little difference of activation energy.

3.3. Models A and B

Comparing model A with model B, it can be deduced that the path in which an H radical attacking on β -C has the lowest

activation energy is the dominant path to yield CH₄ for highly volatile bituminous coal. It is in excellent agreement with the literature, which illustrates that reactions of demethylation as well as the release of groups which cross link ring structures and/or secondary cracking of long chain hydrocarbons within the molecular network of the coal are the major contributor to CH₄ potential in coal [49]. In addition, the activation energy of rate limiting step for H radical attacking on β -CH₃ in model A is 129.8 kJ·mol⁻¹, while the corresponding activation energy of H radical attacking on α -CH₃ in model B is 145.5 kJ·mol⁻¹. Therefore, β -CH₃ is more easily attacked than α -CH₃ by H radical.

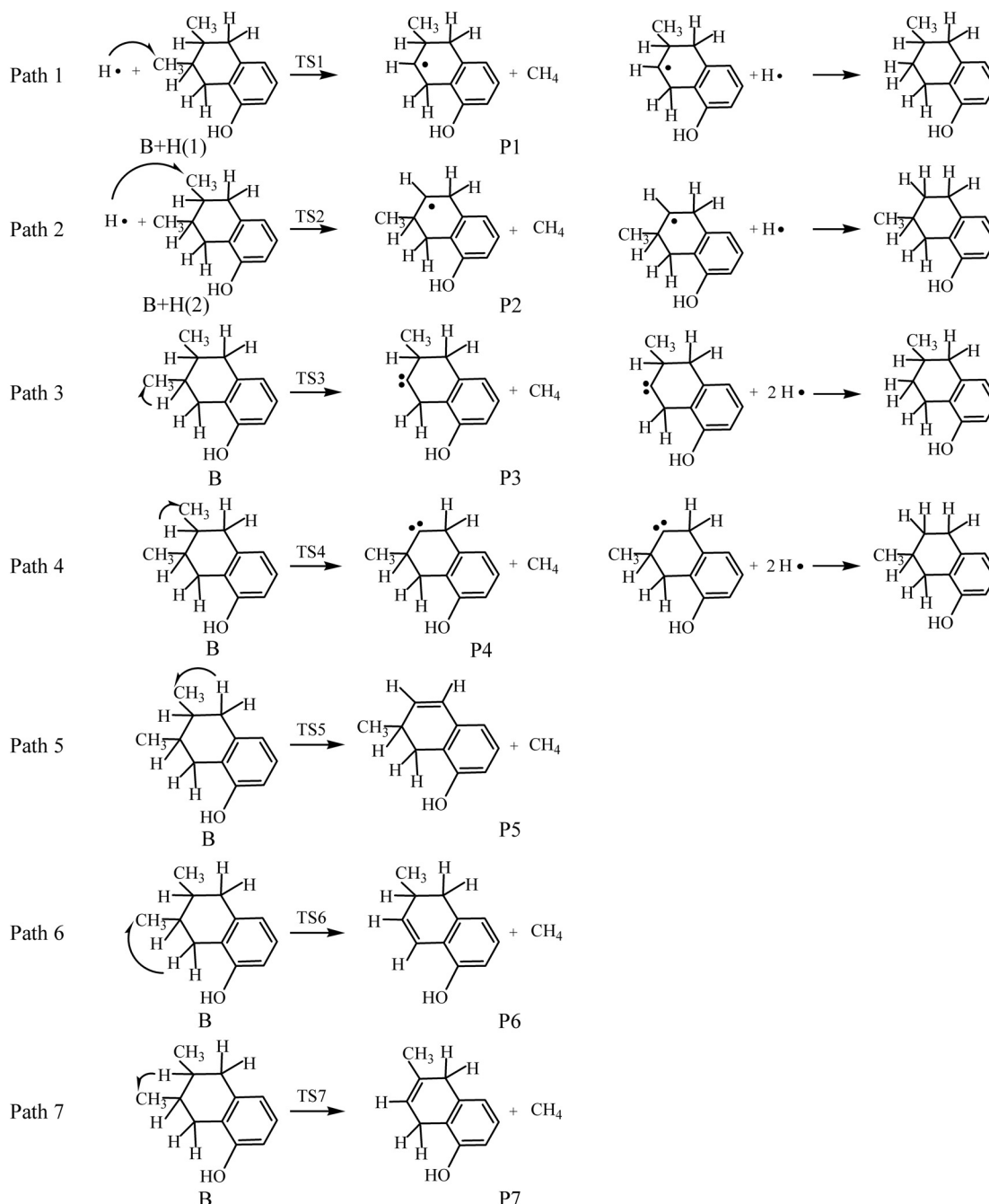


Figure 4. Formation mechanism of CH₄ for model B

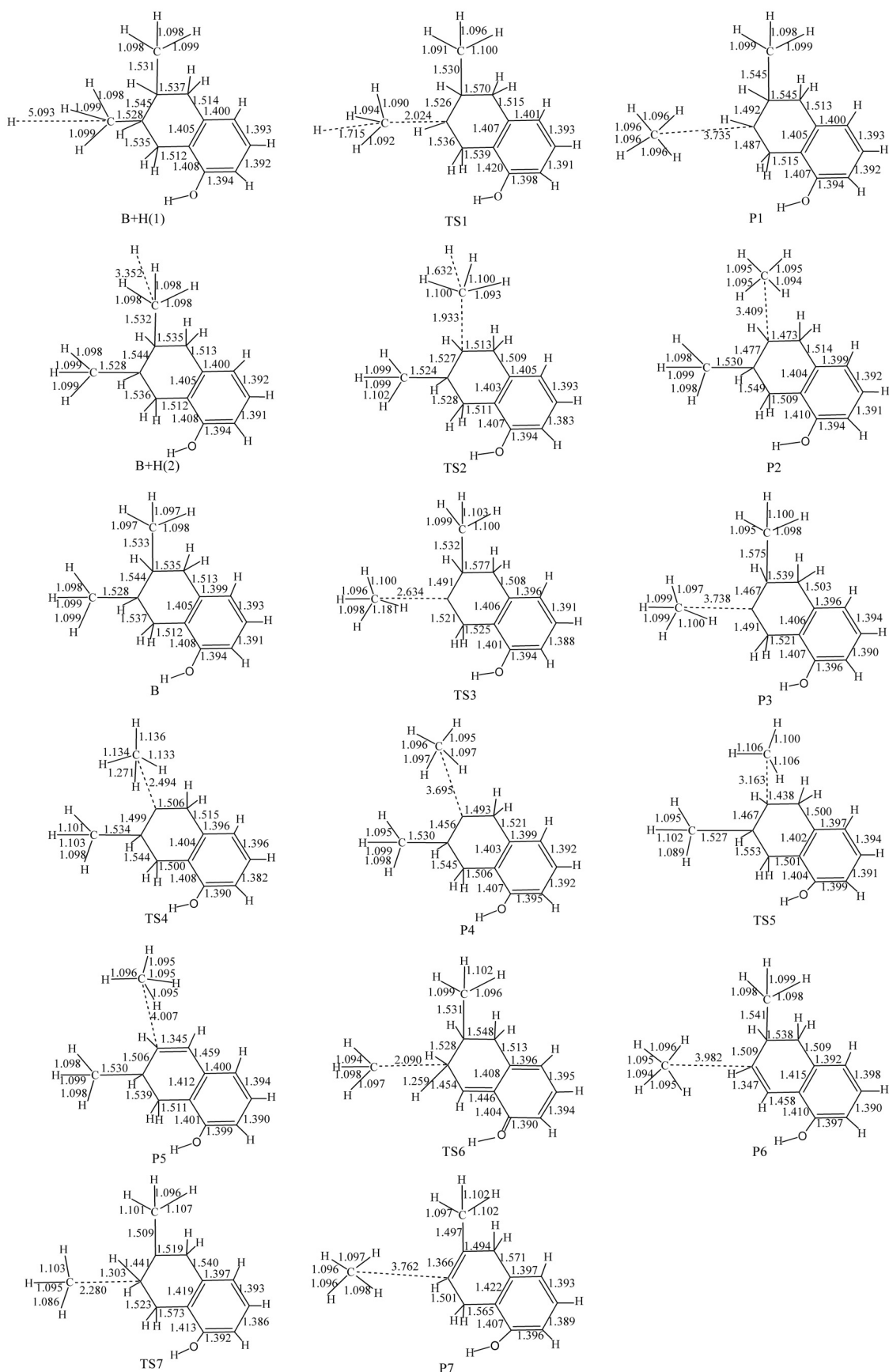


Figure 5. Optimized geometries of all reactants, intermediates, transition states and products during model B pyrolysis

4. Conclusions

By dividing the model of highly volatile bituminous coal (R) into ethylbenzene (A) and 6,7-dimethyl-5,6,7,8-tetrahydro-1-hydroxynaphthalene (B), it is feasible to analyze the formation mechanism of methane in coal. Increasing reaction temperature favors the acceleration of CH₄ formation. The calculated results illustrate that H radicals play an important role in the process of CH₄ formation because activation energies for H-assisted paths are lower than others. Comparing activation energies, it can be concluded that the path in which an H radical attacking on β -C is the dominant path to yield CH₄ for highly volatile bituminous coal. The longer the alkyl side chain is, the easier the C–C bond breaks with the assistance of H radical. A similar chemical environment leads to little difference of activation energy. β -CH₃ is more easily attacked than α -CH₃ by H radical. Information on intramolecular H migration is also compared, that is, the migration of H at α -C to benzene ring is easier than that to β -C; the migration of H at α -C to β -C is easier than that of H at benzene ring to β -C.

Acknowledgements

This work was supported by the Major Projects of National Science and Technology (Grant No. 2011ZX05040-005-002-001), the National Natural Science Foundation of China (Grant No. 21276171 and 21276003), the National Younger Natural Science Foundation of China (Grant No. 21103120) and China Postdoctoral Science Foundation (Grant No. 2012M520608).

References

- [1] Guan P, Wang H Y, Zhang Y X. *Geology*, 2009, 37(10): 915
- [2] Flores R M. *Int J Coal Geol*, 1998, 35(1-4): 3
- [3] Kotarba M J. *Org Geochem*, 2001, 32(1): 163
- [4] Su X B, Lin X Y. *Coalbed Gas Geology*. Beijing: China Coal Industry Publishing House, 2007. 5
- [5] Sun S Q, Li G H, An H T. *Procedia Earth Planet Sci*, 2011, 3: 325
- [6] Su X B, Lin X Y, Liu S B, Zhao M J, Song Y. *Int J Coal Geol*, 2005, 62(4): 197
- [7] Wang B J, Ling L X, Zhang R G, Xie K C. *J China Coal Soc (Meitan Xuebao)*, 2009, 34(9): 1239
- [8] Chen Q L, Yang W M, Teng J W. *Chin J Catal (Cuihua Xuebao)*, 2013, 34(1): 217
- [9] Seo D K, Park S S, Kim Y T, Hwang J, Yu T U. *J Anal Appl Pyrolysis*, 2011, 92(1): 209
- [10] Shi L, Liu Q Y, Guo X J, Wu W Z, Liu Z Y. *Fuel Process Technol*, 2013, 108: 125
- [11] Stanger R, Xie W, Wall T, Lucas J, Mahoney M. *Fuel*, 2013, 103: 764
- [12] Salmon E, van Duin A C T, Lorant F, Marquaire P M, Goddard W A. *Org Geochem*, 2009, 40(12): 1195
- [13] Guo Z Y, Zhang L X, Wang P, Liu H B, Jia J W, Fu X M, Li S D, Wang X G, Li Z, Shu X Q. *Fuel Process Technol*, 2013, 107: 23
- [14] Xie Z L, Feng J, Zhao W, Xie K C, Pratt K C, Li C Z. *Fuel*, 2010, 80(15): 2131
- [15] Chang L P, Xie Z L, Xie K C, Pratt K C, Hayashi J, Chiba T, Li C Z. *Fuel*, 2003, 82(10): 1159
- [16] Huang W, Sun L L, Han P D, Zhao J Z. *J Nat Gas Chem*, 2012, 21(1): 98
- [17] Jia J B, Zeng F G, Li M F, Xie K C. *CIESC J (Huagong Xuebao)*, 2010, 61(12): 3235
- [18] Cui Y B, Wang H, Ran X Q, Wen Z Y, Shi Q Z. *Chin J Org Chem*, 2004, 24(9): 1075
- [19] Ling L X, Zhao L J, Zhang R G, Wang B J. *CIESC J (Huagong Xuebao)*, 2009, 60(5): 1224
- [20] Zhao L J, Ling L X, Zhang R G, Liu X F, Wang B J. *CIESC J (Huagong Xuebao)*, 2008, 59(8): 2095
- [21] Ling L X, Zhang R G, Wang B J, Xie K C. *Chin J Chem Eng*, 2009, 17(5): 805
- [22] Ling L X, Zhang R G, Wang B J, Xie K C. *J Mol Struct*, 2010, 952(1-3): 31
- [23] Ling L X, Zhang R G, Wang B J, Xie K C. *J Mol Struct-Theochem*, 2009, 905(1-3): 8
- [24] Liu S Y, Zhang Z Q, Wang H F. *J Mol Model*, 2012, 18(1): 359
- [25] Delley B. *J Chem Phys*, 1990, 92(1): 508
- [26] Delley B. *J Chem Phys*, 2000, 113(18): 7756
- [27] Perdew J P, Chevary J A, Vosko S H, Jackson K A, Pederson M R, Singh D J, Fiolhais C. *Phys Rev B*, 1992, 46(11): 6671
- [28] Perdew J P, Wang Y. *Phys Rev B*, 1992, 45(23): 13244
- [29] Hohenberg P, Kohn W. *Phys Rev*, 1964, 136(3B): B864
- [30] Halgren T A, Lipscomb W N. *Chem Phys Lett*, 1977, 49(2): 225
- [31] Zhang J Y, Du H C, Wang F, Gong X D, Huang Y S. *J Phys Chem A*, 2011, 115(24): 6617
- [32] Luo Y R. *Handbook of Bond Dissociation Energies in Organic Compounds*. Beijing: Science Press, 2005. 102
- [33] Zeng F G, Jia J B. *Acta Phys-Chim Sin*, 2009, 25(6): 1117
- [34] Jia J B. [PhD Dissertation]. Taiyuan: Taiyuan University of Technology, 2010. 101
- [35] Zhu Z P, Gao J S. *Coal Chemistry*. Shanghai: Shanghai Science and Technology Press, 1984. 129
- [36] Lendvay G. *J Mol Struct-Theochem*, 2000, 501: 389
- [37] Xin J, Sun B M, Zhu H Y, Yin S J, Zhang Z X, Zhong Y F. *J China Coal Soc (Meitan Xuebao)*, 2014, 39(4): 771
- [38] Ju Y W, Jiang B, Hou Q L, Tan Y J, Wang G L, Xiao W J. *Chin Sci Bull*, 2009, 54(1): 88
- [39] Shuai Y H, Peng P A, Zou Y R, Zhang S C. *Org Geochem*, 2006, 37(8): 932
- [40] Das T K. *Fuel*, 2001, 80(4): 489
- [41] Matsuhara T, Hosokai S, Norinaga K, Matsuoka K, Li C Z, Hayashi J. *Energy Fuels*, 2010, 24(1): 76
- [42] Zhu B C. *Chemical Reaction Engineering*. Beijing: Chemical Industry Press, 2006. 24
- [43] Fu X C, Shen W X, Yao T Y, Hou W H. *Physical Chemistry*. Vol. 2. Beijing: Higher Education Press, 2006. 191
- [44] Bauld N L, Bellville D J, Pabon R, Chelsky R, Green G. *J Am Chem Soc*, 1983, 105(8): 2378
- [45] Wang H, Yang H F, Ran X Q, Wen Z Y, Shi Q Z. *J Mol Struct-Theochem*, 2002, 581(1-3): 1
- [46] Mowbray D J, Jones G, Thygesen K S. *J Chem Phys*, 2008, 128(11): 111103
- [47] Ariafard A, Amini M M, Azadmehr A. *J Organomet Chem*, 2005, 690(5): 1147
- [48] Sattelle B M, Shakeri J, Roberts I S, Almond A. *Carbohydr Res*, 2010, 345(2): 291
- [49] Cramer B. *Org Geochem*, 2004, 35(4): 379